

Bicontinuous ion-exchange materials through polymerization-induced microphase separation

David J. Goldfeld[‡], Eric S. Silver[‡], José M. Valdez, Marc A. Hillmyer^{*}

Department of Chemistry, University of Minnesota, Minneapolis, Minnesota, 55455

ABSTRACT: Polymerization-induced microphase separation has been used to prepare solid cross-linked monoliths containing bicontinuous and nanostructured polymer domains. We use this process to fabricate a monolith containing either a negatively or positively charged polyelectrolyte domain inside of the neutral styrene/divinylbenzene derived matrix. First, the materials are made with a neutral *pre*-ionic polymer containing masked charged groups. The monoliths are then functionalized to a charged state by treatment with trimethylamine; small-angle X-ray scattering shows no significant morphological change in the microphase-separated structure upon post-polymerization modification. By exchanging dyes with the counterions in the material, we corroborated the continuity of the charged domains. Using ion-exchange capacity measurements, we estimate the accessible charge within the material based on macroinitiator molar mass and loading.

INTRODUCTION

Polyelectrolytes are polymers containing charges along their chain.¹ They are an important part of many applications involving ion transfer and sequestration, including ion exchange resins and separators in batteries and fuel cells.^{2,3} Their usefulness stems from the generally desirable physical properties of polymers³ and their high fixed charge density.

Practical considerations often require crosslinking polyelectrolytes or functionalizing domains in a microphase-separated system. The ideal material often has high ion conductivity across macroscopic distances, limited transfer of oppositely charged or neutral solutes, and robust mechanical properties.^{4,5} Several studies have attempted to correlate ion conductivity with tunable properties of such polymer systems.^{3,6-9} Conductivity is expected to improve as the charge density in the material increases.¹⁰ However, solvent swelling plays an important role, and ion conductivity in water-containing systems has been shown to initially increase as water content decreases, followed by a significant decrease at water contents that are insufficient to solvate the ions.⁷ Interfacial curvature and dimensions of the charged domains have also proven to be important factors.¹¹ These parameters have been controlled by adjusting the level of functionalization along the polymer chain.¹² But, a series of studies showed that in systems at lower levels of functionalization, the charged monomers gathered into smaller hydrated portions of the domain while the uncharged monomers formed undesirable dry, hydrophobic domains.⁷

Similar roadblocks have been shown in systems that use crosslinking instead of level of functionalization to limit swelling. However, even at high crosslink densities, the polymer still swells because of osmotic driving forces.¹³ Zeldovich and Khokhlov highlighted potential drawbacks in

highly crosslinked systems where inhomogeneities were found in the areas surrounding each crosslink.¹⁴

Polymerization-induced microphase separation (PIMS) is a useful approach to nanostructured monoliths.¹⁵ The synthesis starts with a macroinitiator consisting of a polymer chain end-capped with a reversible addition-fragmentation chain transfer agent (RAFT CTA). The macroinitiator is then dissolved in a mixture of monofunctional and difunctional monomers. An exogenous radical initiator leads to polymer chain extension through controlled radical polymerization. The forming block polymer reaches a molar mass where microphase separation of the macroinitiator from the actively polymerizing matrix occurs. Concurrent crosslinking in the matrix kinetically traps the system, forming a bicontinuous network of percolating nanoscale domains. Variation in the macroinitiator loading and molar mass allows tuning of domain size. When using a degradable polymeric CTA, etching of the macroinitiator domain can lead to high porosities and specific surface areas.¹⁶

PIMS monoliths are desired for applications where synthetic ease and interconnectivity of domains is advantageous. In this communication we use postpolymerization modification with the PIMS synthetic methodology to prepare charged monoliths that contain either positive or negative charges via polyelectrolyte domains percolating through a styrene/divinylbenzene (S/DVB) derived matrix (**Figure 1**). These systems demonstrate high charge density, low swelling, and sequestration of oppositely charged molecules.

RESULTS AND DISCUSSION

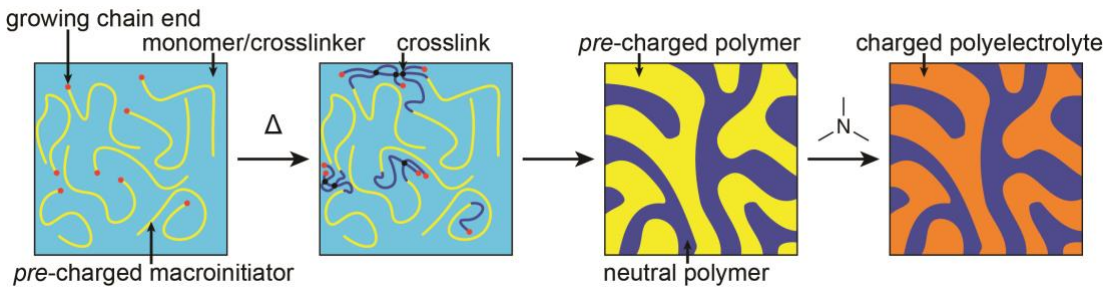


Figure 1: Schematic of polymerization-induced microphase separation to create percolating charged domains.

We previously reported a thin film system containing a neutral ABC triblock polymer consisting of pre-anionic (poly(*n*-propyl styrene sulfonic ester)), a neutral styrenic block, and pre-cationic (poly(*p*-vinylbenzyl chloride)) [PVBC] blocks to produce three distinct domains that could be converted through exposure to a trialkylamine solution to both positive and negative charges.¹⁷ Here, we use that general strategy in a PIMS strategy to create bicontinuous, nanostructured, and charged materials.

n-Octyl styrene sulfonic ester (oSSE) monomer was synthesized following a similar method to the synthesis of *n*-propyl styrene sulfonic ester previously reported,¹⁸ substituting 1-octanol for 1-propanol. The oSSE monomer has not been previously reported; full characterization is included in the Supporting Information. oSSE was polymerized using a trithiocarbonate RAFT CTA as an initiator,¹⁹ which produced poly(*n*-octyl styrene sulfonate ester) (PoSSE) samples of controlled molar masses and $\mathcal{D} < 1.5$. Two molar masses were used in this study, $M_n = 21$ and $55 \text{ kg}\cdot\text{mol}^{-1}$. PVBC homopolymer was prepared in an analogous manner to produce two macroinitiators of comparable molar masses $M_n = 24$ and $46 \text{ kg}\cdot\text{mol}^{-1}$.

The selected macro-chain transfer agent (MacroCTA) was dissolved in a trichloro(3,3,3-trifluoropropyl)silane-treated vial containing a 4:1 molar ratio of S:DVB at either 20 or 30 wt% loadings (samples referred to as MacroCTA- M_n -loading). MacroCTA loadings below 20 wt% did not consistently result in monoliths with interconnected domains. In addition, the high molar mass PoSSE macroinitiator was only sparingly soluble in the S/DVB mixture, even at 20 wt%. Thus, in the case of PoSSE, we emphasize the use of the low molar mass material. A small amount of AIBN was added to the vials and the mixtures were purged with argon, sealed, and quiescently heated in an oil bath at 70°C for 24 h. After cooling, the vials were broken apart and the monoliths were subjected to reduced pressure overnight to remove any unreacted S/DVB. The as-synthesized samples are optically transparent with a yellow tint due to the trithiocarbonate end groups (Figure 4); they were then sanded flat and polished to remove any macroscopic surface imperfections.

Small-angle X-ray scattering (SAXS) of the monoliths showed a broad peak in all of the samples, consistent with previous disordered PIMS systems (Figure 2).¹⁶ The principle scattering peak, q^* , corresponded to domain spacings of 19 and 54 nm for the PoSSE-21k-20 and PoSSE-55k-20 materials, respectively. Similarly, the q^* for the PVBC containing PIMS indicated domain spacings of 15 and 43 nm for the PVBC-24k-20 and PVBC-46k-20 samples,

respectively. A peak was expected for the PoSSE PIMS since we have previously shown that other poly(styrene sulfonic esters) will microphase separate from polystyrene in related block polymer systems. In the case of PVBC, however, there have been no examples of a PS-PVBC block polymer showing microphase separation. The fact that PVBC PIMS scatter in our system indicates that PVBC and PS are characterized by a small positive Flory-Huggins interaction parameter. At some molar mass and/or degree of crosslinking in the PIMS system, the PS block on the end of the growing PVBC chains reaches a molar mass or level of crosslinking that is high enough to drive microphase separation.

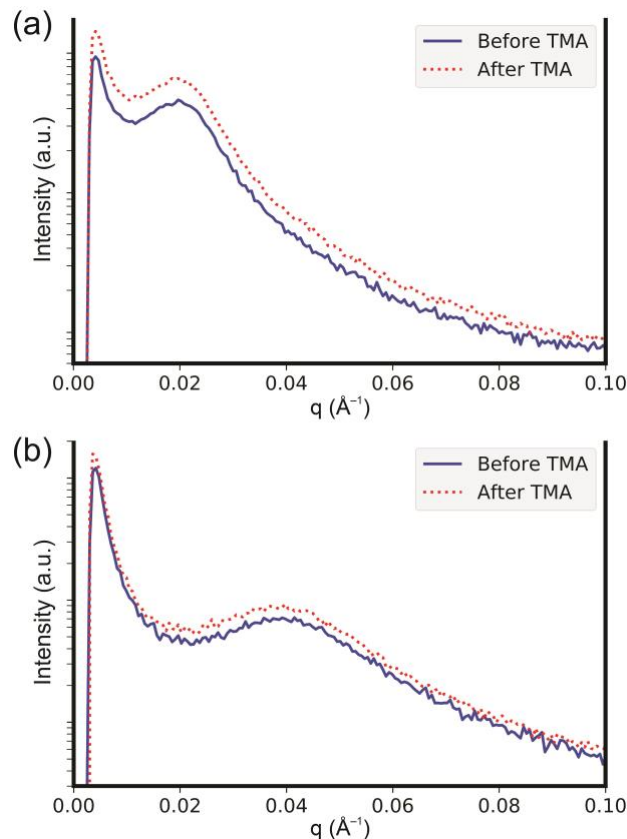


Figure 2: Transmission SAXS data of (a) a representative PoSSE-55k-20 PIMS (solid blue line) before and (dotted red line) after TMA exposure and (b) PVBC-24k-20 (solid line) before and (dashed line) after TMA exposure.

Attenuated total reflectance infrared spectroscopy (ATR-IR) suggests the MacroCTA backbones were largely

unaffected during the PIMS process as the C-Cl stretch of the PVBC and the asymmetric S-O-C stretch of the sulfonic ester were retained. To convert the neutral macroinitiator domains into charged polyelectrolytes, the monoliths were soaked in an aqueous solution containing 45 wt% trimethylamine (TMA). ATR-IR showed complete disappearance of the same C-Cl and S-O-C peaks in the PVBC and PoSSE monoliths, respectively (**Figure 3**). ATR-IR data was acquired on various points of both the exterior and interior of the monolith and corroborated complete functionalization throughout the sample. Transmission SAXS measurements showed negligible change in the observed scattering pattern or peak position, indicating morphological integrity through TMA treatment (**Figure 2**).

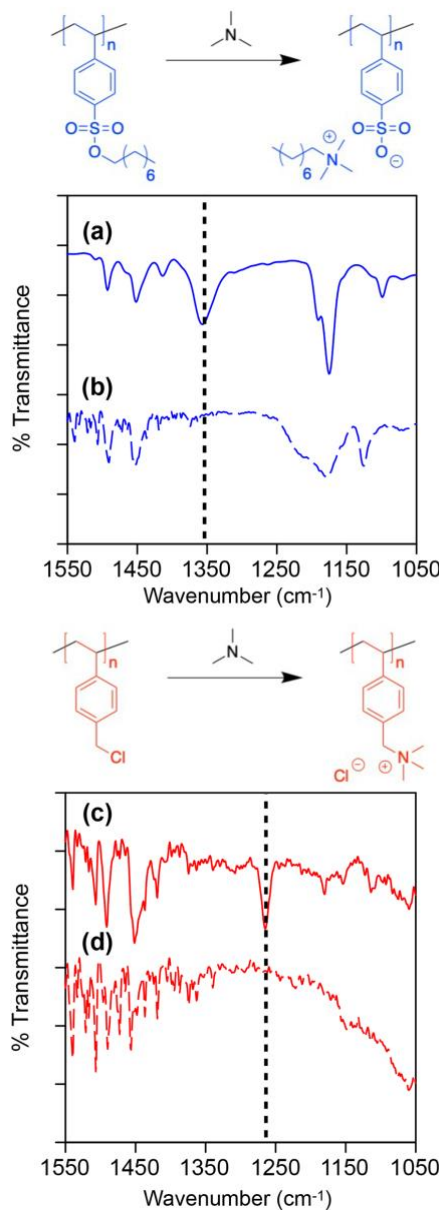


Figure 3: ATR-IR of (a) unfunctionalized and (b) TMA exposed PoSSE-62k-30 PIMS and (c) unfunctionalized and (d) TMA exposed PVBC-24k-20 PIMS.

By ATR-IR, the monoliths functionalized after a few hours upon exposure to TMA, even over significant thicknesses (millimeters). We attribute this rather rapid conversion to the functionalized and ionic polymer drawing aqueous amine solution into the polyelectrolyte domain, directly exposing the deeper parts of the sample to base solution. The monoliths may react faster than the 24 h time frame we used, but the exposure time was held constant to help ensure quantitative conversion.

After functionalization, the monoliths became more hydrophilic but only slightly swelled in the presence of water. Although the outer dimensions of the sample remained essentially constant, the mass increased by around 5% after soaking in aqueous media. This low level of swelling did, however, result in some loss in mechanical integrity, and some monoliths, especially those with 30 wt% macroinitiator loading, often cracked or broke into pieces after functionalization in aqueous media, especially as the swollen monoliths were subsequently dried. Similarly, exposure to trimethylamine revealed macrophase separation and inhomogeneities in both the higher molar mass PoSSE-55k-20 and PoSSE-55k-30 samples.

We further confirmed the successful functionalization using ion exchange with charged dyes. Each PIMS sample was soaked in two different phosphate-buffered solutions, one containing negatively charged methyl red dye and the other positively charged toluidine blue dye. The unfunctionalized PIMS samples remained transparent and only a small amount of dye appeared to physisorb onto the surface. Further, the monoliths were the same mass before and after soaking. In contrast, the charged monoliths again increased in mass by around 4% from their dry weight, indicative of swelling. The monoliths clearly absorbed the complementary-charged dye, emerging either dark orange or dark blue through the thickness of the material depending on which dye was absorbed (**Figure 4**).

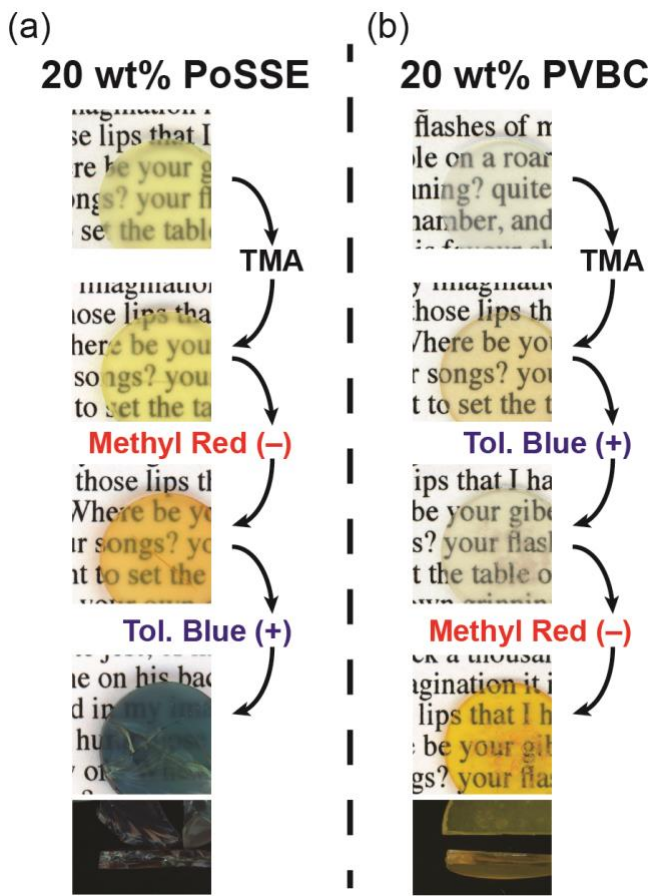


Figure 4: Images of (a) PoSSE-21k-20 and (b) PVBC-24k-20 monoliths as made, after functionalization with TMA, and after exposure to positively and negatively charged dyes.

Ultraviolet-visible absorption spectroscopy (UV-vis) was used to determine the amount of dye absorbed into the monolith. Before functionalization, the PIMS monoliths absorbed a statistically negligible amount of dye after 24 h (**Figure S28-S29**). After functionalization, the negatively charged PoSSE monoliths absorbed a vast majority of the positively charged toluidine blue dye in solution and little of the negatively charged methyl red. The positively charged PVBC monoliths displayed the opposite behavior, absorbing almost all of the negatively charged methyl red in solution, but not the positively charged toluidine blue. Fracturing the monoliths showed blue (for the PoSSE PIMS) or orange (for the PVBC PIMS) through the thickness of the sample (**Figure 4**). These data are consistent with the PIMS samples consisting of percolating, connected domains that allow the charged dyes to permeate through the material. This also indicates that despite the low swelling in the monoliths, the passive ion exchange kinetics allow some diffusion across several millimeters in a 24 h timespan.

The theoretical charge density of the materials is high. The sulfonic ester and the vinylbenzyl chloride guarantee a single charge per monomer with near 100% functionalization according to IR analysis. As an example, the PoSSE-21k-30 monolith contains 0.3 g of PoSSE polymer in a 1 g sample. After functionalization, the sample therefore contains about 0.95 mmol of charged monomers in each gram of dry monolith.

Because the crosslinked matrix has a fixed geometry, the volume of the PoSSE domain should not significantly change after functionalization to the negatively-charged poly(styrene sulfonic acid) with the corresponding tetraalkylammonium counterion. If we then assume that the density of the PoSSE is the same as the density of the matrix (assumed to be 1 g/cm³), we calculate there to be approximately 2 charges·nm⁻³ within the polyelectrolyte domain.

Such a high charge density is difficult to achieve in soft materials; common ion exchange polymers have a dry charge density around 0.6 charge·nm⁻³.²⁰ Deformation and expansion under swelling further decreases the charge density. In the materials we have prepared, however, the glassy and crosslinked matrix retains the shape and the covalent anchoring of the polyelectrolyte prevents leaching of the charged domain into the surrounding space. These restrictions force the volume to remain essentially constant, even in the presence of excess water. Based on the ~5% swelling we measure in PoSSE-21k-30, we estimate that the monoliths absorb only 2.9 water molecules per charge. Water content at such a low level may be incapable of fully solvating the ions in the polyelectrolyte domain; common ion exchange polymers swell at least 10%.²⁰ In addition, because every monomer contains a charge, we expect the water to be evenly distributed throughout the polyelectrolyte domain.

We sought to verify the number of charges in the monoliths by measuring their ion exchange capacity (IEC). To do this, we functionalized PoSSE monoliths with TMA and crushed them into a powder to increase the accessible surface area. We then soaked the powder in 0.1 M H₂SO₄ to exchange the tetraalkylammoniums that result upon functionalization for protons. After the acid soak, the crushed material was rinsed with water multiple times and was then soaked in 1 M NaCl solution to exchange the protons for sodium ions. The salt solution was then titrated with sodium hydroxide to neutral using phenolphthalein as an indicator. The IEC indicated there was about half the expected number of charges in the monolith (0.4 mmol charge/g monolith for PoSSE-62k-30 compared to a theoretical ion capacity of ~1 mmol charge/g monolith).

We suspect this discrepancy could be caused by several factors. The first is the kinetics of passive exchange. With the swelling as low as the mass indicates, diffusion is likely quite slow to the center of the monoliths without any driving force. Secondly, the functionalization of the sulfonic ester with amines may be preventing efficient ion exchange with harder ions (protons).²¹ If the softer ammoniums are staying bound to the sulfonic acid groups, even a high local concentration of protons will have trouble exchanging. Finally, the samples used were relatively small (less than 150 mg) which decreases the precision of the pH titration.

A similar trend was seen in the IEC of the PVBC PIMS. Instead of soaking in acid, the functionalized PIMS was soaked in 0.1 M NaOH solution to displace the chloride ions with hydroxide ions. After soaking in water to remove excess ions, the monolith was soaked in 1 M NaCl solution to release the hydroxide ions. The pH was then titrated to neutral using HCl and phenolphthalein as the indicator. Again, this showed a lower ion exchange capacity than

theoretically predicted (0.8 mmol charges/g monolith for PVBC-24k-30 compared to the theoretical 2 mmol charge/g monolith). We again attribute this to the kinetics of the passive exchange, which are likely restricting the accuracy of the measurement.

CONCLUSIONS

Through the use of polymerization induced microphase separation, we have shown the ability to create polyelectrolyte-containing monoliths with high charge densities. Using two different macroinitiators, we formed monoliths with either positive or negative charges. By then exposing them to oppositely charged dyes, we showed through passive ion exchange that the domains percolate throughout the thickness of the monolith and contain only positive or negative fixed charges. We measured the ion concentration in an effort to show the extremely high ion densities and low levels of solvation. The ease of fabrication makes these materials good candidates for use in battery separators and separations membranes, among other applications.²⁻⁵

ASSOCIATED CONTENT

Supporting Information

The Supporting Information is available free of charge on the ACS Publications website. Materials, instrumentation, experimental methods, NMR spectra, dn/dc measurements, SEC chromatograms, thermal analyses, SAXS scattering plots, and UV-vis absorption spectra (PDF)

AUTHOR INFORMATION

Corresponding Author

* hillmyer@umn.edu

Author Contributions

The manuscript was written through contributions of all authors. / All authors have given approval to the final version of the manuscript. / [†]These authors contributed equally.

Funding Sources

The authors acknowledge the National Science Foundation for financial support of this work (DMR-2003454)

Notes

Any additional relevant notes should be placed here.

ACKNOWLEDGMENT

Parts of this work were carried out in the Characterization Facility, University of Minnesota, which receives partial funding support from the National Science Foundation (NSF) through the MRSEC program.

ABBREVIATIONS

S, styrene; PS, polystyrene; VBC, *p*-vinylbenzyl chloride; PVBC, poly(*p*-vinylbenzyl chloride); oSSE, *n*-octyl styrene sulfonic ester); PoSSE, poly(*n*-octyl styrene sulfonic ester); DVB, divinylbenzene; TMA, trimethylamine; AIBN, azobisisobutyronitrile; ATR-IR, attenuated total reflectance infrared spectroscopy; SAXS, small-angle X-ray scattering; UV-vis, ultraviolet-visible spectroscopy; CTA, chain transfer agent;

REFERENCES

- (1) Jenkins, A. D.; Kratochvíl, P.; Stepto, R. F. T.; Suter, U. W. Glossary of Basic Terms in Polymer Science (IUPAC Recommendations 1996). *Pure Applied Chemistry* **1996**, *68*, 2287-2311.
- (2) Mauritz, K. A.; Moore, R. B. State of Understanding of Nafion. *Chem. Rev.* **2004**, *104*, 4535-4586.
- (3) Kraytsberg, A.; Ein-Eli, Y. Review of Advanced Materials for Proton Exchange Membrane Fuel Cells. *Energy Fuels* **2014**, *28*, 7303-7330.
- (4) Lee, H.; Yanilmaz, M.; Toprakci, O.; Fu, K.; Zhang, X. A review of recent developments in membrane separators for rechargeable lithium-ion batteries. *Energy Environ. Sci.* **2014**, *7*, 3857-3886.
- (5) Harry, K. J. Lithium dendrite growth through solid polymer electrolyte membranes. PhD Thesis, University of California, Berkeley: Berkeley, CA, 2016.
- (6) Chen, X. C.; Kortright, J. B.; Balsara, N. P. Water Uptake and Proton Conductivity in Porous Block Copolymer Electrolyte Membranes. *Macromolecules* **2015**, *48*, 5648-5655.
- (7) Kim, S. Y.; Park, M. J.; Balsara, N. P.; Jackson, A. Confinement Effects on Watery Domains in Hydrated Block Copolymer Electrolyte Membranes. *Macromolecules* **2010**, *43*, 8128-8135.
- (8) Jeon, C.; Han, J. J.; Seo, M. Control of Ion Transport in Sulfonated Mesoporous Polymer Membranes. *ACS Appl. Mater. Interfaces* **2018**, *10*, 40854-40862.
- (9) Chen, L.; Hallinan, D. T., Jr.; Elabd, Y. A.; Hillmyer, M. A. Highly Selective Polymer Electrolyte Membranes from Reactive Block Polymers. *Macromolecules* **2009**, *42*, 6075-6085.
- (10) Wang, P.; Anderko, A.; Young, R. D. Modeling Electrical Conductivity in Concentrated and Mixed-Solvent Electrolyte Solutions. *Ind. Eng. Chem. Res.* **2004**, *43*, 8083-8092.
- (11) Jackson, G. L. Nanoconfined Water and Water-mediated Ion Transport in Model Lyotropic Liquid Crystals. PhD Thesis, University of Wisconsin-Madison: Madison, WI, 2018.
- (12) Serpico, J. M.; Ehrenberg, S. G.; Fontanella, J. J.; Jiao, X.; Perahia, D.; McGrady, K. A.; Sanders, E. H.; Kellogg, G. E.; Wnek, G. E. Transport and Structural Studies of Sulfonated Styrene-Ethylene Copolymer Membranes. *Macromolecules* **2002**, *35*, 5916-5921.
- (13) Rumyantsev, A. M.; Pan, A.; Ghosh Roy, S.; De, P.; Kramarenko, E. Y. Polyelectrolyte Gel Swelling and Conductivity vs Counterion Type, Cross-Linking Density, and Solvent Polarity. *Macromolecules* **2016**, *49*, 6630-6643.
- (14) Zeldovich, K. B.; Khokhlov, A. R. Osmotically Active and Passive Counterions in Inhomogeneous Polymer Gels. *Macromolecules* **1999**, *32*, 3488-3494.
- (15) Seo, M.; Hillmyer, M. A. Reticulated Nanoporous Polymers by Controlled Polymerization-Induced Microphase Separation. *Science* **2012**, *336*, 1422-1425.
- (16) Schulze, M. W.; Hillmyer, M. A. Tuning Mesoporosity in Cross-Linked Nanostructured Thermosets via Polymerization-Induced Microphase Separation. *Macromolecules* **2017**, *50*, 997-1007.
- (17) Goldfeld, D. J.; Silver, E. S.; Radlauer, M. R.; Hillmyer, M. A. Synthesis and Self-Assembly of Block Polyelectrolyte Membranes through a Mild, 2-in-1 Postpolymerization Treatment. *ACS Appl. Polym. Mater.* **2020**, *2*, 817-825.
- (18) Kolomanska, J.; Johnston, P.; Gregori, A.; Domínguez, I. F.; Egelhaaf, H.-J.; Perrier, S.; Rivaton, A.; Dagron-Lartigau, C.; Topham, P. D. Design, synthesis and thermal behaviour of a series of well-defined clickable and triggerable sulfonate polymers. *RSC Advances* **2015**, *5*, 66554-66562.
- (19) Moad, G.; Chong, Y. K.; Postma, A.; Rizzardo, E.; Thang, S. H. Advances in RAFT polymerization: the synthesis of polymers with defined end-groups. *Polymer* **2005**, *46*, 8458-8468.
- (20) *AmberLite™ HPR9200 Cl Product Data Sheet*, 1st ed.; Dupont, 2019; pp 1-4.

(21) Boyd, G. E.; Larson, Q. V. The Binding of Quaternary Ammonium Ions by Polystyrenesulfonic Acid Type Cation Exchangers. *J. Am. Chem. Soc.* **1967**, *89*, 6038–6042.

Table of Contents Graphic

